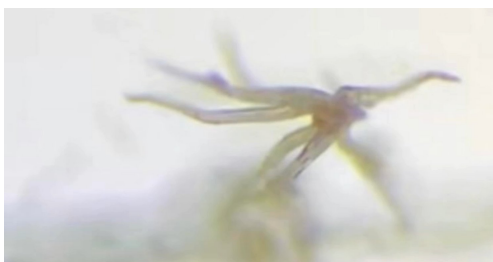


Strange objects / substances in Vaccines

Capt. Wardrobe - Oct 2021

Video: Stew Peters & Dr. Carrie Madej Reveal "Living Organism" Inside Covid Vials

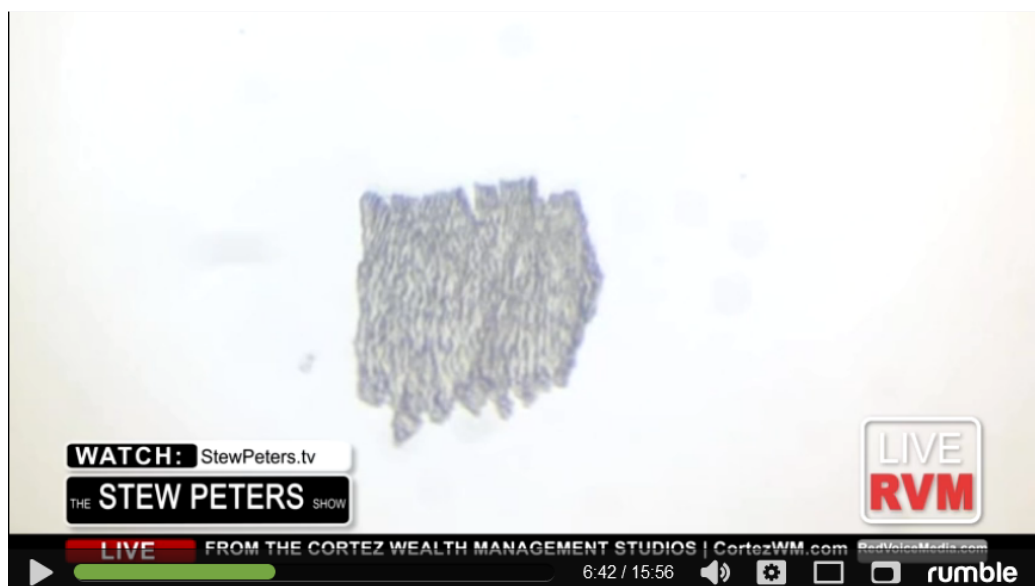


OCTOBER 13, 2021

In neurodegenerative diseases, brain immune cells have a 'ravenous appetite' for sugar

by German Center for Neurodegenerative Diseases







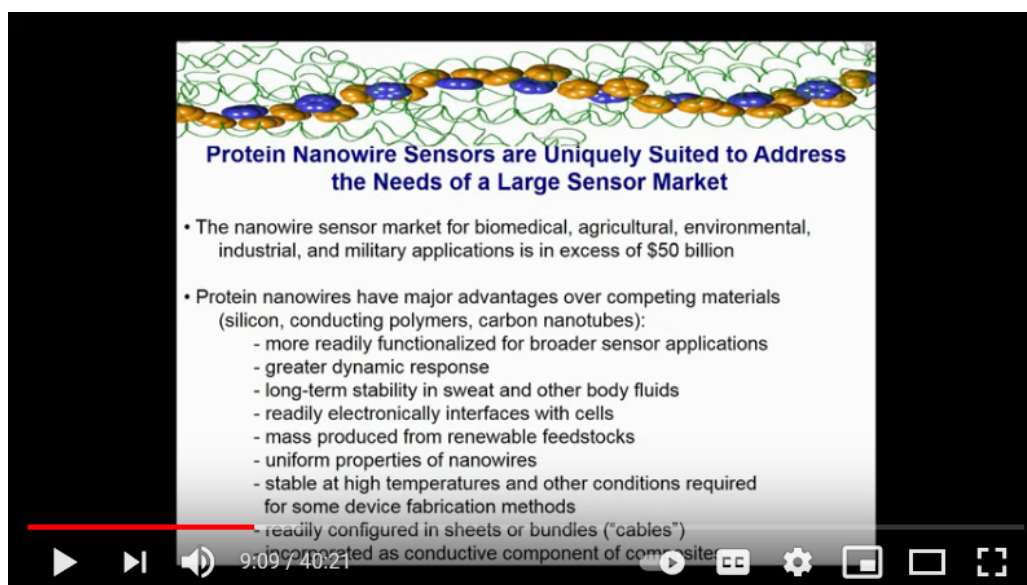
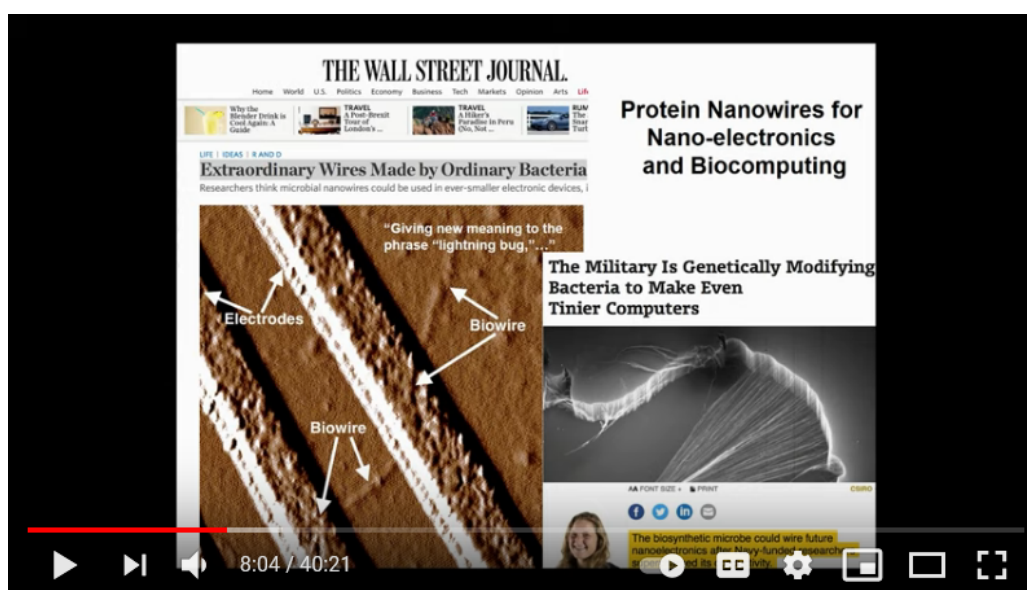




Screenshots from Dr Derek Lovelys talk

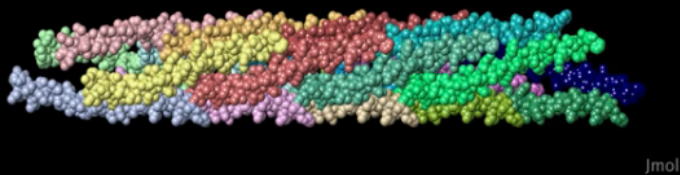
"Protein nanowires for sensing, energy harvesting & wiring cells to electronics"



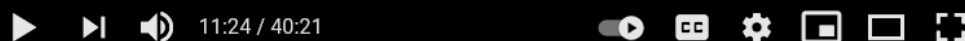


Key Points About *Geobacter* Protein Nanowires

1. They assemble from a single monomer peptide of ca. 60 amino acids to form a wire 3 nm in diameter and 10-30 μm long.



Malvankar, N.S., M. Vargas, K.P. Nevin, P.-L. Tremblay, K. Evans-Lutterodt, D. Nykypanchuk, E. Martz, M.T. Tuominen, and D.R. Lovley. 2015. Structural basis for metallic-like conductivity in microbial nanowires. *mBio* 6:e00084-15.



Key Points About *Geobacter* Protein Nanowires

3. Protein Nanowires have metallic-like conductivity- a new paradigm for biological proteins

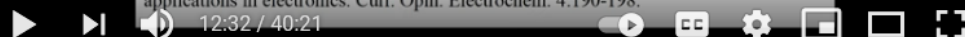
Hopping or tunneling among **localized** charge carriers (cytochromes) is the known mechanism for biological electron transport



In metallic-like conduction, charges are spread across the molecules (**Delocalized**)

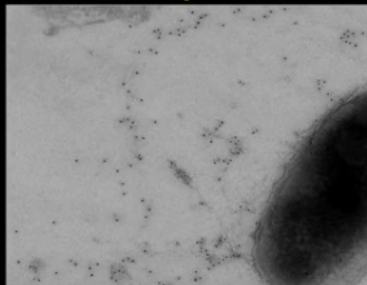


Lovley, D. R. 2017. Electrically conductive pili: biological function and potential applications in electronics. *Curr. Opin. Electrochem.* 4:190-198.



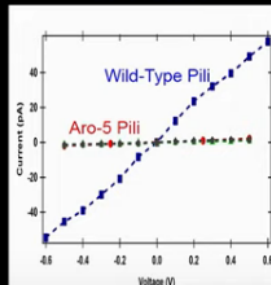
Strain Aro-5 Produces Synthetic Pili with 1000-Fold Lower Conductivity than Wild-Type but with Properly Localized Outer Surface Cytochromes

Transmission Electron Micrograph of Cell with Immunogold-Labeled Outer-Surface Cytochrome OmcS

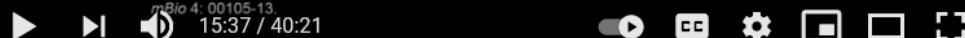


Vargas et al. 2013. Aromatic amino acids required for pili conductivity and long-range extracellular electron transport in *Geobacter sulfurreducens*. *mBio* 4: 00105-13.

Current-Voltage Plots of Individual Wild-Type and Aro-5 Pili

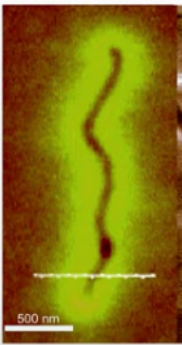


R.Y. Adhikari et al. 2016. Conductivity of individual *Geobacter* pili. *RSC Advances* 6:8354-8357



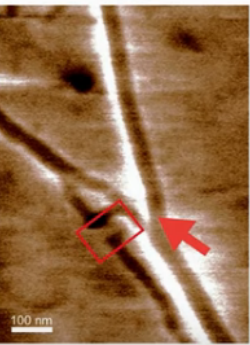
Electrostatic Force Microscopy Revealed that Charge Propagation in e-Pili is Similar to that in Carbon Nanotubes

Carbon Nanotube



500 nm

e-Pili



100 nm

Malvankar, N. S., S. E. Yalcin, M. T. Tuominen, and D. R. Lovley. 2014. Visualization of charge propagation along individual pili proteins using ambient electrostatic force microscopy. *Nature Nanotechnology* 9:1012-1017 .

15:52 / 40:21

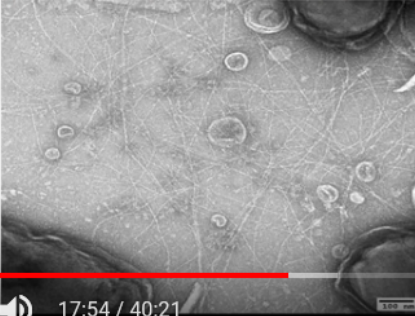
Expression of *G. metallireducens* Pili in *G. sulfurreducens*

PilA Amino Acid Sequences

G. metallireducens Sequence is Shorter and Contains More Aromatics

	10	20	30	40	50	60			
<i>G. sulfurreducens</i>	FTLI	ELIVVA	IGILA	AIPOFS	AYRVKAYNSA	SSDLRN	LKTALES	FADDQ	TYPPES
<i>G. metallireducens</i>	FTLI	ELIVVA	IGILA	AIPOFA	AYRQKAFNSA	ESDLKNT	KNLES	YYSEH	QFYPN--


TEM Demonstrating Abundant Pili Expression




Tan, Y., R. Y. Adhikari, N. S. Malvankar, J. E. Ward, T. L. Woodard, K. P. Nevin, and D. R. Lovley. 2017. Expressing the *Geobacter metallireducens* PilA in *Geobacter sulfurreducens* yields pili with exceptional conductivity. *mBio* 8:e02203-16.

17:54 / 40:21

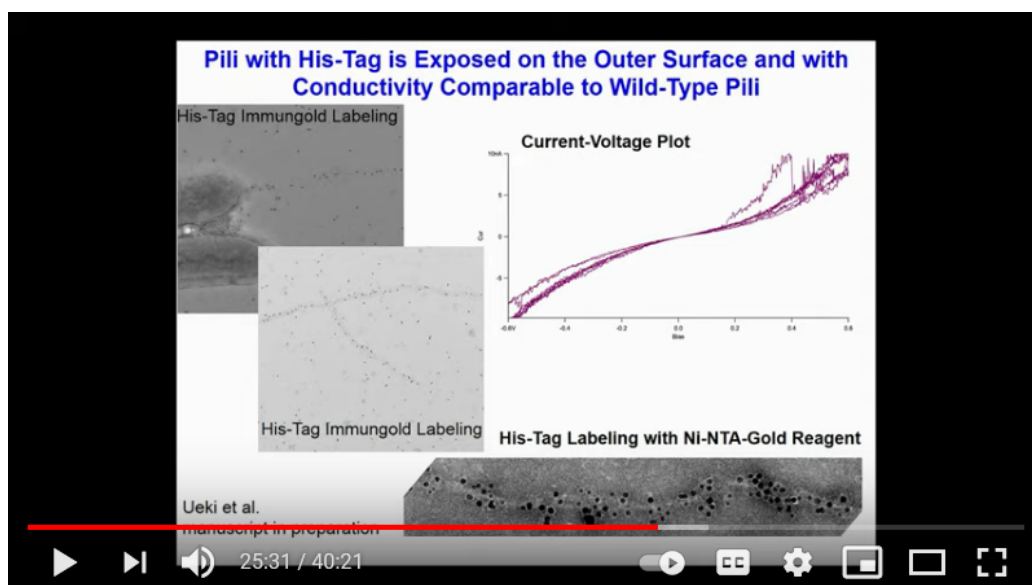
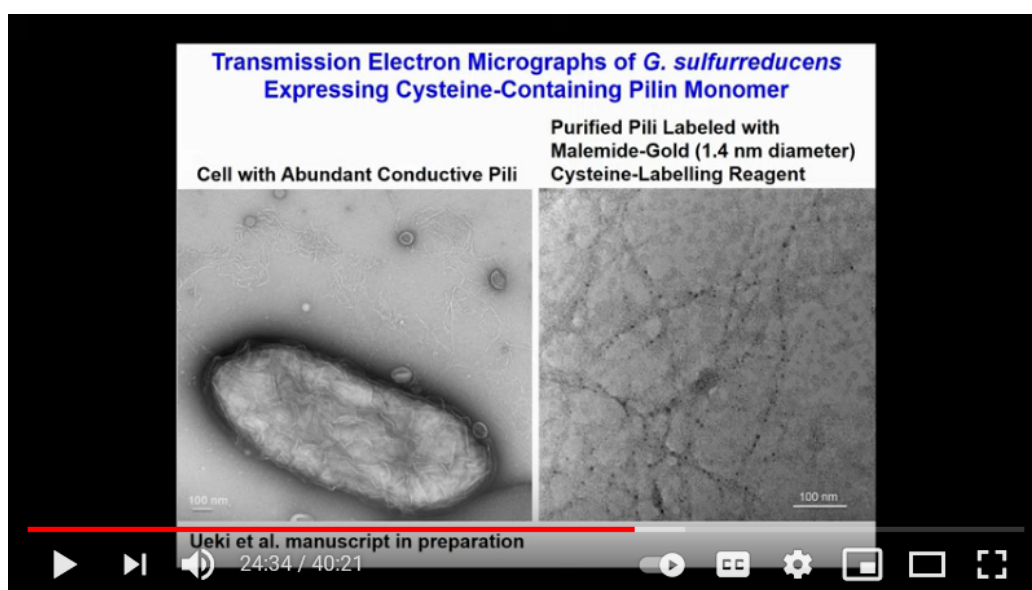
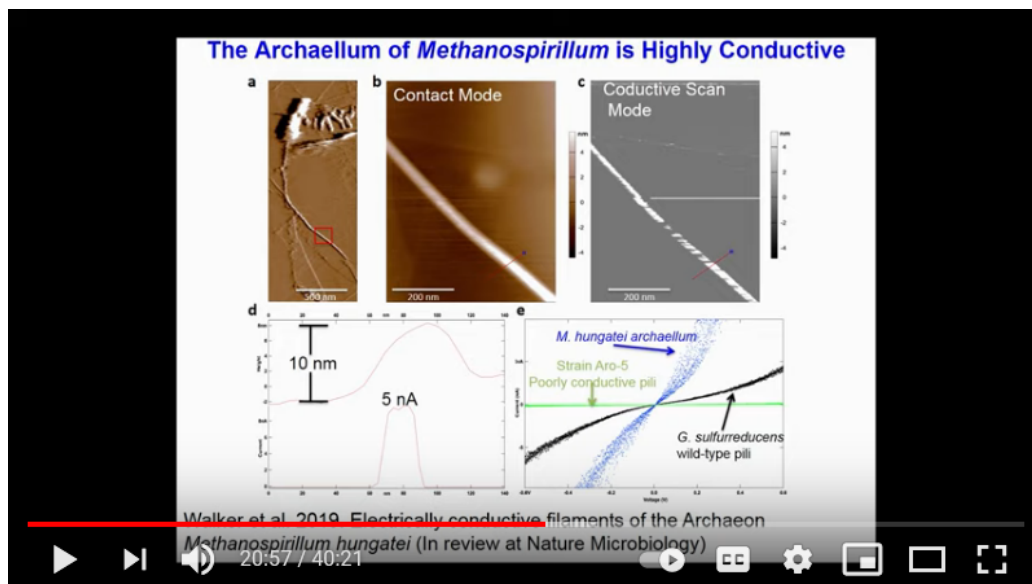
Modeling Approach Based on First Principles of Protein Assembly also Suggests that π - π Stacking is Possible





Xiao et al. 2016. Low energy atomic models suggesting a pilus structure that could account for electrical conductivity along the length of *Geobacter sulfurreducens* pili. *Scientific Reports* 6:23385.

19:19 / 40:21



Key Points About *Geobacter* Protein Nanowires

6. Composite conductive materials can be fabricated with protein nanowires.

Drop-casting

(a) (b) (c) (d)

(e) (f)

Y.-I. Sun et al. 2018. Conductive composite materials fabricated with microbially produced protein nanowires. *Small* 14:10.1002/smll.201802624

Figure (e) shows cyclic voltammograms for different MNW contents. The x-axis is Voltage (V) from -10 to 10, and the y-axis is Current Density ($\mu\text{A cm}^{-2}$) from -10 to 10. Multiple curves are shown, with an arrow indicating that current density increases with MNW content.

Figure (f) shows the conductivity (S cm^{-1}) on a logarithmic scale (from 10^{-10} to 10^7) versus the MNW/PVA Weight Fraction (%) from 0 to 12. The data points follow a power-law fit: $\sigma = \sigma_0(\phi - \phi_c)^t$, with $\phi_c = -0.2\%$ and $t \sim 1.0$.

The Conductivity of MNW/PVA Composites Increases with Decreasing pH

(a) pH 10.5 pH 7.0 pH 1.5

(b) (c)

Y.-I. Sun et al. 2018. Conductive composite materials fabricated with microbially produced protein nanowires. *Small* 14:10.1002/smll.201802624

Figure (a) shows SEM images of MNW/PVA composites at pH 10.5, pH 7.0, and pH 1.5. The images show a transition from a smooth surface at high pH to a more textured, conductive surface at low pH.

Figure (b) shows cyclic voltammograms for different pH levels (pH 1.5, pH 7.0, pH 10.5). The x-axis is Voltage (V) from -6 to 6, and the y-axis is Current Density (A cm^{-2}) on a logarithmic scale from 10^{-7} to 10^{-2} . The current density increases significantly at lower pH.

Figure (c) shows the conductivity (S/cm) on a logarithmic scale (from 10^{-7} to 10^3) versus pH from 0 to 12. The conductivity increases sharply as pH decreases.

Nanowires Self-Assemble in Hexane into 2-D 'Tapes' and Retain High Conductivity

500 nm 100 nm

Yun-Lu Sun et al. (unpublished)

The inset shows a cyclic voltammogram with Current (μA) on the y-axis (from -1.0 to 1.0) and Voltage (mV) on the x-axis (from -100 to 100). Multiple curves are shown, labeled Point 1 through Point 6, all showing high conductivity.

